Immunology & Cell Biology 2018; **96**: 128–136
www.wileyonlinelibrary.com/journal/icb

OUTSTANDING OBSERVATION

GPR65 inhibits experimental autoimmune encephalomyelitis through CD4$^+$ T cell independent mechanisms that include effects on iNKT cells

Rushika C Wirasinha[1,2], Dipti Vijayan[1,2], Nicola J Smith[2,3], Grant P Parnell[4], Alexander Swarbrick[2,5], Robert Brink[1,2], Cecile King[1,2], Graeme Stewart[4], David R Booth[4] & Marcel Batten[1,2]

1 Immunology Division, Garvan Institute of Medical Research, Sydney, NSW, Australia
2 St. Vincent's Clinical School, University of New South Wales, Sydney, NSW, Australia
3 Molecular Pharmacology Group, Victor Chang Cardiac Research Institute, Darlinghurst, NSW, Australia
4 Centre for Immunology and Allergy Research, Westmead Institute for Medical Research, University of Sydney, Westmead, NSW, Australia
5 The Kinghorn Cancer Centre and Cancer Research Division, Garvan Institute of Medical Research, Darlinghurst, NSW, Australia

Keywords
Autoimmune disease, CD4$^+$ T cells, cytokine, experimental autoimmune encephalomyelitis, G Protein-Coupled Receptor 65, invariant NKT cells, multiple sclerosis.

Correspondence
Marcel Batten, 384 Victoria St. Darlinghurst, NSW 2010, Australia.
E-mail: m.batten@garvan.org.au

Present address
Rushika C Wirasinha, Infection and Immunity Program, Biomedicine Discovery Institute and Department of Biochemistry and Molecular Biology, Monash University, Clayton, Vic, Australia
Dipti Vijayan, Immunology in Cancer and Infection Laboratory, QIMR Berghofer Medical Research Institute, Herston, Queensland, Australia

Received 18 September 2017;
Revised 14 November 2017;
Accepted 15 November 2017

doi: 10.1111/imcb.1031

Immunology & Cell Biology 2018; **96**: 128–136

Abstract

The G protein-coupled receptor 65 (*GPR65*) gene has been genetically associated with several autoimmune diseases, including multiple sclerosis (MS). GPR65 is predominantly expressed in lymphoid organs and is activated by extracellular protons. In this study, we tested whether GPR65 plays a functional role in demyelinating autoimmune disease. Using a murine model of MS, experimental autoimmune encephalomyelitis (EAE), we found that *Gpr65*-deficient mice develop exacerbated disease. CD4$^+$ helper T cells are key drivers of EAE pathogenesis, however, *Gpr65* deficiency in these cells did not contribute to the observed exacerbated disease. Instead, *Gpr65* expression levels were found to be highest on invariant natural killer T (iNKT) cells. EAE severity in *Gpr65*-deficient mice was normalized in the absence of iNKT cells (*CD1d*-deficient mice), suggesting that GPR65 signals in iNKT cells are important for suppressing autoimmune disease. These findings provide functional support for the genetic association of GPR65 with MS and demonstrate GPR65 signals suppress autoimmune activity in EAE.

INTRODUCTION

Newly identified G protein-coupled receptors (GPCRs) are attractive therapeutic targets due to receptor-ligand specificity, their cell membrane localization and the discrete distribution of individual GPCRs in the body. As a testament to their suitability as drug targets, an estimated 36% of existing, marketed pharmaceuticals act at GPCRs.[1] Genome wide association studies have identified the G protein-coupled receptor *65 (GPR65)* locus to be associated with multiple sclerosis (MS)[2,3], as well as type 1 diabetes,[4] ankylosing spondylitis,[5] inflammatory bowel diseases[6,7] and rheumatoid arthritis.[8] The GPR65 locus also contains the *GALC* gene and these two genes are in tight linkage disequilibrium.[2,3] Thus, genetic association studies alone are unlikely to identify

which gene is driving increased risk of MS. Expression of the inflammatory bowel disease-associated risk variant of *GPR65* (rs3742704) or null deletion of *GPR65* both resulted in autophagy defects, consistent with the loss of function of GPR65 in the disease-associated haplotype.[9] Functional studies are required to determine the relevance and importance of GPR65 in MS.

Gpr65-deficient mice display no overt phenotype prior to immunological challenge, nor any changes in antibody production in response to T-dependent or T-independent antigens.[10] *Gpr65*-deficient mice develop exacerbated disease in models of arthritis and delayed-type hypersensitivity.[11] These mice also exhibit increased immune cell recruitment, IL17A production and adverse outcomes in a model of myocardial infarction.[12] Mutation of *Gpr132*, a *Gpr65* family member, leads to the development of a lupus-like autoimmune condition in mice.[13] These previous observations support the idea that GPR65 controls immunological processes relevant to MS, independent of unstimulated T-cell phenotype and antibody production.

GPR65 encodes an acid (proton) sensing GPCR[14,15] for which the biological outcomes of signaling are incompletely understood. Local tissue acidosis, due to glycolysis, is a hallmark of inflammation. Acidic pH has been reported in the CNS during experimental autoimmune encephalomyelitis (EAE) (pH 6.6 compared with 7.4 in healthy CNS)[16] and lactate has been detected in MS patient brain biopsies.[17] There is evidence that GPR65 signaling could control numerous aspects of immune function through the adenylate cyclase pathway. Increasing acidity results in GPR65-dependent Gαs-mediated activation of adenylate cyclase and leads to the accumulation of cAMP in multiple primary cell types including eosinophils,[18] macrophages,[19] and thymocytes.[20] In leukocytes, cAMP/PKA can influence many cellular functions including activation, motility and cytokine production.[21]

Here, we test the hypothesis that GPR65 regulates EAE development. Our data point to a key regulatory role for GPR65 in demyelinating autoimmunity, at least partially through effects on iNKT cells.

RESULTS

Gpr65-deficient mice develop exacerbated EAE

The $Gpr65^{gfp/gfp}$ mouse line has GFP spliced into the second exon of the *Gpr65* gene, generating a complete deletion of *Gpr65* with GFP as a reporter of GPR65 expression.[10] To test the functional relevance of GPR65 in demyelinating autoimmune disease, we induced "active" EAE in groups of $Gpr65^{gfp/gfp}$ and $Gpr65^{+/+}$ mice by immunizing with MOG_{35-55} peptide in incomplete Freund's adjuvant supplemented with heat-killed *Mycobacterium tuberculosis* (*M. Tb*). In our colony, inclusion of pertussis toxin led to highly lethal form of disease (d.n.s); we therefore omitted pertussis toxin in our disease induction strategy. Omission of pertussis toxin also avoided disrupting Gαi association with GPCRs,[22] although GPR65 is not thought to associate with Gαi.[15] This strategy produced EAE with mild severity, allowing for the detection of any changes in disease in the absence of GPR65.

Mice were monitored for 30 days after immunization. Average disease scores were higher in the $Gpr65^{gfp/gfp}$ group compared to $Gpr65^{+/+}$ controls and area under the curve (AUC) analysis indicated that $Gpr65^{gfp/gfp}$ mice developed significantly exacerbated disease (Figure 1a), with individual $Gpr65^{gfp/gfp}$ animals reaching significantly higher peak clinical scores than $Gpr65^{+/+}$ mice (Figure 1b). The median onset of disease was 17 days for $Gpr65^{gfp/gfp}$ mice and 22 days for $Gpr65^{+/+}$ mice. A trend for increased incidence of mice developing symptoms of disease was observed in $Gpr65^{gfp/gfp}$ mice, although this did not reach statistical significance (Figure 1c). Thus, in contrast to a recent report, in which adoptively transferred $Gpr65^{gfp/gfp}$ $CD4^+$ T cells were unable to confer disease,[23] we found that $Gpr65^{gfp/gfp}$ mice were indeed susceptible to typical active EAE induction and developed more severe disease than their wildtype counterparts.

Loss of *Gpr65* expression in MOG_{35-55}-specific $CD4^+$ T cells does not significantly exacerbate EAE development in an adoptive transfer model

In the EAE model, demyelinating disease is induced by activated MOG_{35-55} peptide-specific $CD4^+$ T cells.[24] To analyze the effects of *Gpr65* deficiency within $CD4^+$ T cells in the context of EAE, we generated mixed bone marrow (BM) chimeras comprising 50% $Gpr65^{+/+}$ or $Gpr65^{gfp/gfp}$ (Thy1.2 expressing) BM mixed with 50% WT C57BL6 (Thy1.1 expressing) BM. In the steady-state, $Gpr65^{gfp/gfp}$ $CD4^+$ T cells repopulate irradiated hosts and differentiate normally (Figure 2a).

To test $CD4^+$ T cell function upon challenge, mixed BM chimeras were immunized with MOG_{35-55} in CFA (as for EAE induction) and the draining inguinal LN and central nervous system (CNS) infiltrating leukocytes collected at D15 post immunization, corresponding to the time of disease onset. Tissues were subjected to MOG_{35-55} re-stimulation *ex vivo* to allow quantitation of intracellular cytokines in antigen-specific $CD4^+$ T cells. Intracellular staining was performed to test IL-17, IFNγ and Foxp3 expression in $CD4^+$ T cells. Expression

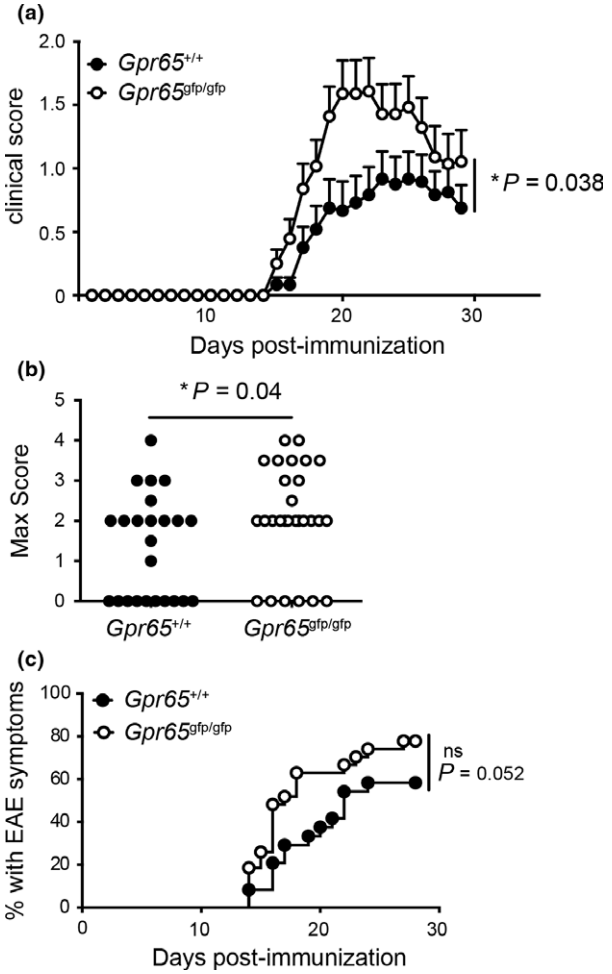

Figure 1. *Gpr65*-deficient mice develop exacerbated EAE. $Gpr65^{+/+}$ ($n = 24$) or $Gpr65^{gfp/gfp}$ ($n = 28$) mice were immunized in the flank with 50 μg MOG_{35-55} in incomplete Freund's adjuvant containing 400 μg *M. Tb*. Clinical symptoms of paralysis were monitored over 30 days. **(a)** Average clinical score in each group, bars indicate s.e.m. **(b)** Maximum clinical scores reached, each symbol represents an individual mouse. **(c)** Incidence of EAE symptoms over time. Data are pooled from two independent cohorts. For clinical scores, $P < 0.05$ was determined by area under the curve for each mouse and groups compared using an unpaired *t*-test. For maximum scores, $P < 0.05$ was determined using an unpaired *t*-test. For incidence, $P < 0.05$ was determined using a Gehan-Breslow-Wilcoxon test. EAE, experimental autoimmune encephalomyelitis.

of these factors in either WT ($CD45.2^+Thy1.2^+$) or $Gpr65^{gfp/gfp}$ ($CD45.2^+Thy1.2^+$) $CD4^+$ T cells was compared to the expression observed in the C57BL6 ($CD45.2^+Thy1.1^+$) $CD4^+$ T cells present in the same host mouse. The ratio in each mouse was calculated, as this overcomes the variation in disease severity between host mice. Raw values are provided in Supplementary figure 1. The data indicate that there are no T cell intrinsic differences in IL-17, IFNγ or Foxp3 expression in $Gpr65^{gfp/gfp}$ $CD4^+$ T cells. Likewise, when $CD4^+$ T cells from nonchimeric $Gpr65^{gfp/gfp}$ and $Gpr65^{+/+}$ mice were MOG_{35-55} restimulated *ex vivo*, no significant differences in cytokine production were observed (d.n.s).

MOG_{35-55} specific $CD4^+$ T cells from 2D2.Tg mice were used to specifically test the function of $Gpr65^{gfp/gfp}$ $CD4^+$ cells *in vivo* in the EAE setting. In this transfer model of EAE, 2D2 MOG_{35-55} specific $CD4^+$ T cells were transferred into immunologically replete wildtype recipients. 2D2.Tg $Gpr65^{+/+}$ or 2D2.Tg $Gpr65^{gfp/gfp}$ donor cells induced comparable disease in recipients (Figure 2c). Proliferation of CTV-labeled, adoptively transferred 2D2.Tg T cells was similar 3 days after immunization with MOG_{35-55} in CFA (Figure 2d). Thus, $CD4^+$ T cell differentiation and function, and the anti-MOG response appears to be intact in $Gpr65^{gfp/gfp}$ mice.

Since GPR65 activates MEK/ERK[25] and enhances the survival of eosinophils and lymphoma cells,[18,25] we also tested whether survival was effected in $Gpr65^{gfp/gfp}$ $CD4^+$ T cells. Indeed, a survival defect was observed in $Gpr65^{gfp/gfp}$ $CD4^+$ T cells in culture either with or without anti-CD3/anti-CD28 stimulation (Figure 2e and f).

GPR65 is highly expressed by iNKT cells and *Gpr65* deficiency does not alter the course of EAE in the absence of iNKT cells

Since changes in the conventional $CD4^+$ T cell anti-MOG response could not explain exacerbated EAE in $Gpr65^{gfp/gfp}$ mice, we next investigated *Gpr65* expression in other immune cells. The GFP reporter in $Gpr65^{gfp}$ knock-in mice has been used previously to show expression of *Gpr65* in the stages of developing thymocytes as well as broadly in mature populations of $CD4^+$ and $CD8^+$ T cells, B cells, granulocytes, macrophages, NK ($CD3^-/DX5^+$) cells and DC.[10] We extended this to investigate the regulation of GPR65 during T-cell activation and in additional cell types. The intensity of the GFP reporter in heterozygous mice ($Gpr65^{+/gfp}$) was used to characterize expression (Figure 3a). Since we observed that the $CD4^+CD44^+CD62L^{lo}$ (effector $CD4^+$ cell) gate contained up to 40% iNKT cells in immunologically naïve mice in our colony, we were careful to use αGalCer-CD1d tetramer to differentiate iNKT cells and conventional T (T-conv) cells. *Gpr65* was widely expressed, with reporter GFP detected in all immune cells tested (Figure 3a and b). *Gpr65* expression was high in DN2 thymocytes, NK cells, DC, γδ T cells and was most highly expressed by iNKT cells, which had approximately twice the GFP level of naïve $CD4^+$ T cells (Figure 3a and b). By contrast, effector $CD4^+$ T cells had slightly reduced GFP signal compared to naïve $CD4^+$ cells (Figure 3a and b). *Gpr65* mRNA quantitation in iNKT cells showed an even more

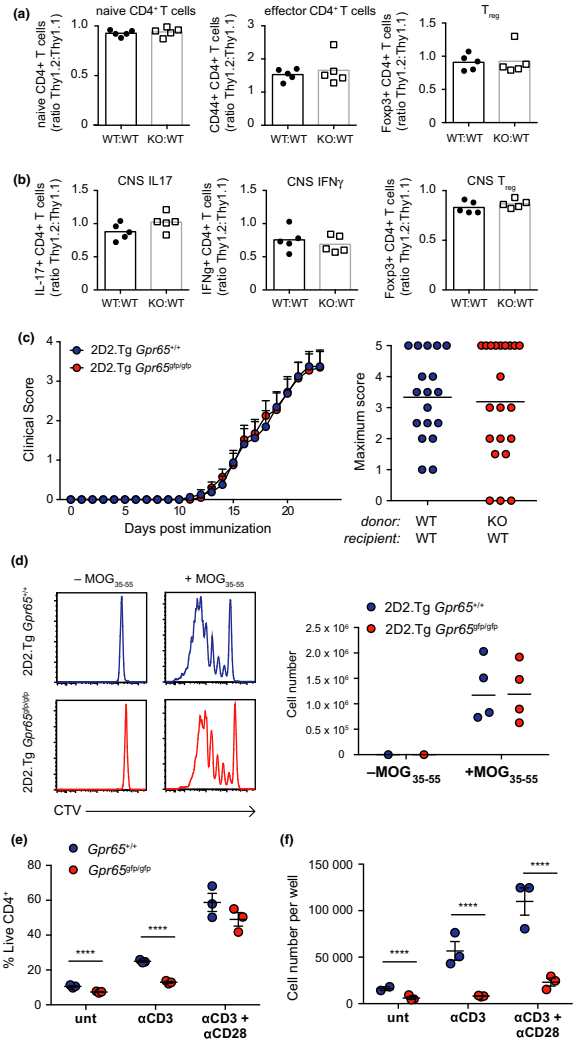

Figure 2. CD4$^+$ T cells do not contribute to the exacerbated EAE observed in *Gpr65*-deficient mice. **(a-b)** 50:50 mixed BM chimeras were generated using 50% *Gpr65*$^{gfp/gfp}$ BM (CD45.2$^+$Thy1.2$^+$) mixed with 50% Thy1.1 congenic WT BM (CD45.2$^+$Thy1.1$^+$). Control group mice were generated with 50% *Gpr65*$^{+/+}$ BM (CD45.2$^+$Thy1.2$^+$) mixed with 50% Thy1.1 congenic WT BM (CD45.2$^+$Thy1.2$^+$). Recipient mice were irradiated CD45.1 mice. **(a)** Reconstitution was assessed at 8 weeks post-transfer and the percentage of CD4$^+$ naïve, effector and regulatory T cells in the *Gpr65*$^{+/+}$ (closed circles) or *Gpr65*$^{gfp/gfp}$ (open squares) gate is shown relative to the CD45.2$^+$Thy1.1$^+$ WT donor cells in the same mouse. **(b)** Mixed BM chimeras were immunized with MOG_{35-55} as in Figure 1 and CNS infiltrating leukocytes were harvested at day 15 post immunization. Cells were re-stimulated with 100 μg mL^{-1} MOG_{35-55} *ex vivo* for 24 h. The percentage of cytokine positive cells in the *Gpr65*$^{+/+}$ (closed circles) or *Gpr65*$^{gfp/gfp}$ (open squares) gate is shown relative to the CD45.2$^+$Thy1.1$^+$ WT donor cells in the same mouse. Data are representative of three independent experiments. No statistically significant differences were observed using a *t*-test. (C and D) 2D2.Tg *Gpr65*$^{+/+}$ or 2D2.Tg *Gpr65*$^{gfp/gfp}$ CD4$^+$ T cells were transferred into WT.CD45.1$^+$ recipients, simultaneously immunized with MOG_{35-55} as in Figure 1. **(c)** Average clinical score for each group (left panel) over 26 days, bars indicate s.e.m. Maximum scores reached by individual animals (right panel; each symbol represents an individual mouse, bars indicate the mean). 2D2.Tg *Gpr65*$^{+/+}$, $n = 8$; 2D2.Tg *Gpr65*$^{gfp/gfp}$, $n = 10$. Data is representative of two independent experiments. **(d)** 2D2.Tg *Gpr65*$^{+/+}$ and 2D2.Tg *Gpr65*$^{gfp/gfp}$ CD4$^+$ naïve T cells were sorted, labeled with CTV and equal numbers of each were mixed. WT.CD45.1$^+$ recipient mice received a total of 5×10^5 cells. Recipients were simultaneously immunized as in **(c)**. Mice were sacrificed on day 3 post-transfer and iLN harvested for flow cytometric analysis. Representative CTV plots and the cell number recovered from each mouse for unimmunized (−MOG_{35-55}) and immunized (+MOG_{35-55}) mice. Each symbol represents an individual mouse, bars indicate the mean. No statistically significant differences were observed. The data presented are representative of two independent experiments. **(e & f)** Sorted naïve CD4$^+$ T cells from *Gpr65*$^{+/+}$ or *Gpr65* $^{gfp/gfp}$ mice were left untreated (unt) or stimulated with anti-CD3 alone (αCD3) or along with anti-CD28 (αCD3 + αCD28) for 48 h. **(e)** Live 7AAD-negative cells as a percentage of the total lymphocyte gate and **(f)** calculation of total live cell number per well. Each point represents an experimental replicate. Representative of four independent experiments. Bars indicate mean ± s.d. Unpaired *t*-test ****$P < 0.0001$. BM, bone marrow; EAE, experimental autoimmune encephalomyelitis. [Color figure can be viewed at wileyonlinelibrary.com]

striking increase, with at least 40-fold higher *Gpr65* mRNA observed in sorted iNKT cells compared with any of the T-conv cell subsets tested (Figure 3c). Investigation of GFP expression in iNKT cell subsets, divided based on CD4 and NK1.1 expression, revealed uniformly high expression (Supplementary figure 2). These data collectively demonstrate that *Gpr65* is expressed widely on leukocytes, including all types of peripheral T cells tested, and the expression was particularly high on innate and innate-like lymphocytes.

It was noted that effector $CD4^+$ and $CD8^+$ T cells had reduced GFP expression relative to naïve T cells (Figure 3a and b). We therefore examined the expression of GFP in iNKT cells at day 10 after the induction of EAE. In line with the observations in T-conv cells, GFP MFI in iNKT cells was reduced during EAE (Figure 3d). However the GFP levels in iNKT cells remained higher than those observed in $CD44^+$ $CD4^+$ T-conv cells (Figure 3d).

Given the elevated expression of *Gpr65* in iNKT cells, the impact of *Gpr65* deficiency on the steady state populations within the thymus and in peripheral lymphoid organs was investigated. The percentages and total cell numbers of iNKT were comparable between $Gpr65^{+/+}$ and $Gpr65^{gfp/gfp}$ mice within thymus, spleen and iLN (Figure 3e).

TCR-mediated activation of iNKT cells via αGalCer administration during EAE suppressed disease severity in groups of both $Gpr65^{+/+}$ and $Gpr65^{gfp/gfp}$ mice (d.n.s). However, the interpretation of this data is complicated by the fact that all iNKT cell subsets, including those producing IFNγ, IL-4 and IL-17, are highly stimulated by αGalCer, skewing the cytokine profile independently of GPR65. Also, the TCR mediated nature of the activation differs from conventional EAE where iNKT cells are activated indirectly.[26] We therefore used an iNKT deficient model.

Development of iNKT cells is dependent upon interaction with cells expressing the MHC-like molecule CD1d. To assess whether $Gpr65^{gfp/gfp}$ mice displayed exacerbated EAE in the absence of iNKT cells, $CD1d^{-/-}$ $Gpr65^{gfp/gfp}$ mice were generated. $CD1d^{-/-}$ $Gpr65^{gfp/gfp}$ and $CD1d^{-/-}$ $Gpr65^{+/+}$ mice exhibited similar disease severity (Figure 3f). The observation of disease exacerbation in WT $Gpr65^{gfp/gfp}$ mice, but not $CD1d^{-/-}$ $Gpr65^{gfp/gfp}$ mice suggests that loss of *Gpr65* in iNKT cells could contribute to the pathogenesis of EAE.

DISCUSSION

The increased severity of EAE in the absence of GPR65 provides functional evidence to support the genetic association of GPR65 in autoimmune demyelinating disease.[2,3] Our data indicate that GPR65 plays a protective role during EAE, since exacerbated EAE was observed in *Gpr65*-deficient mice compared with wildtype controls. Our data contrast with a published study, in which wildtype or *Gpr65* deficient $CD4^+$ T cells (from the same strain used in our investigation[10]) were isolated and transferred into $Rag1^{-/-}$ recipients, and EAE induced by immunization two weeks later.[23] That study found that disease was delayed in mice that received *Gpr65* deficient $CD4^+$ T cells, compared with those that received wildtype cells.[23] The differing effect on disease in that model could be a consequence of low numbers of Gpr65 deficient $CD4^+$ T cells in $Rag1^{-/-}$ recipient mice after the parking period, as we have noted a survival defect of naïve $CD4^+$ T cells from *Gpr65*-deficient mice (Figure 2e and f). GPR65 has been shown to enhance cell survival in eosinophils[18] and lymphoma cell lines through MEK/ERK activation.[25] Therefore it is possible that the "parked" $CD4^+$ T cells, which would have been undergoing homeostatic proliferation in the $Rag1^{-/-}$ host in the 2 weeks prior to immunization,[27] may have proliferated or survived less efficiently than wildtype counterparts. In addition, recipient mice in that study lacked B cells, $CD8^+$ T cells and iNKT cells. We have demonstrated that *Gpr65*-deficient mice develop exacerbated disease in a system with minimal manipulation and in immunologically replete animals. Furthermore, our analysis of mixed BM chimeric mice provides strong evidence for normal function of $Gpr65^{gfp/gfp}$ $CD4^+$ T cells in EAE. In line with our findings, GPR65 was also required to attenuate inflammation in models of arthritis[11] and myocardial infarction.[12]

Our investigation uncovered strikingly high expression of GPR65 in iNKT cells, along with normalized EAE levels in *Gpr65*-deficient mice in the absence of iNKT cells. *Gpr65* mRNA levels were ~40 fold higher in iNKT cells compared with naïve T cells. We were not able to confirm changes at the protein level due to a lack of specific anti-GPR65 antibodies. The percentage of iNKT cells in various organs was not altered in the absence of *Gpr65*, however this does not preclude changes in iNKT cell function. Innate-like T cells such as iNKT cells, mucosa-associated invariant T (MAIT) cells and γδT cells exist in a pre-activated state and can have potent effects in EAE through the early production of cytokines.[28-30] Although iNKT cells are less numerous in human tissue, iNKT and MAIT cells have been found within MS lesions, their numbers negatively correlate with disease and functional data suggest an immunosuppressive role for these cells.[29-33] These data are consistent with a homeostatic role for GRP65 in acidic conditions, preventing excessive immune response through regulation of iNKT cells. The $Gpr65^{gfp}$ reporter data presented here also shows high levels of expression in other innate-like lymphoid cells such γδT cells and NK cells. MAIT cells are infrequent in mice and

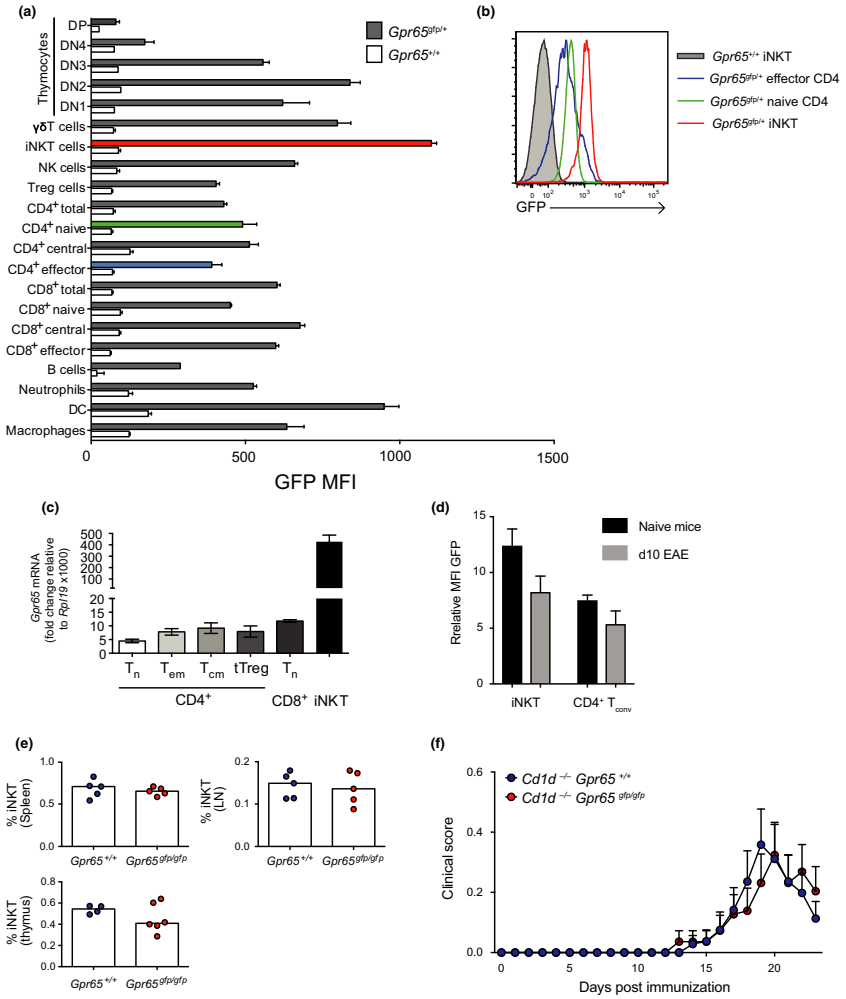

Figure 3. iNKT cells express high levels of *Gpr65* and contribute to the exacerbated EAE observed in *Gpr65-deficient* mice **(a)** Mean fluorescence intensity (MFI) of the GPR65 GFP reporter was determined by flow cytometry, gating various immune cell populations of *Gpr65*$^{gfp/+}$ mice (filled bars) and compared to autofluorescence in the same populations in *Gpr65*$^{+/+}$ mice (empty bars). Populations were defined by the following markers: Thymocytes DN1 (CD4$^-$CD8$^-$CD44$^+$CD25$^-$), DN2 (CD4$^-$CD8$^-$CD44$^+$CD25$^+$), DN3 (CD4$^-$CD8$^-$CD44$^-$CD25$^+$), DN4 (CD4$^-$CD8$^-$CD44$^-$CD25$^-$) and DP (CD4$^+$CD8$^+$CD44$^-$CD25$^-$), γδ T cells (CD3$^+$γδTCR$^+$), iNKT cells (CD3$^+$CD1dtet$^+$), NK cells (CD3$^-$NK1.1$^+$), Treg (CD4$^+$CD25$^+$), CD4$^+$ and CD8$^+$ naïve (CD1dtet$^-$CD62L$^+$CD44$^-$), effector (CD1dtet$^-$CD62L^{lo}CD44$^+$) and central memory (CD1dtet$^-$CD62L$^+$CD44$^+$) T cells, B cells (B220$^+$), neutrophils (CD11b$^+$Ly6G$^+$), DC (CD11c$^+$) and macrophages (CD11b$^+$). Bars indicate the mean of 2-3 individual mice and S.D. **(b)** Representative histogram overlays for GFP levels in *Gpr65*$^{gfp/+}$ iNKT cells (red line), CD4$^+$ naïve (green line) and effector T cells (blue line). Background fluorescence in *Gpr65*$^{+/+}$ iNKT cells is given (grey filled histogram). **(c)** Relative *Gpr65* mRNA levels in FACS purified wildtype CD4$^+$ naïve (Tn), CD4$^+$ central memory (Tcm), CD4$^+$ effector memory (Tem), CD8$^+$ naïve (Tn) and iNKT cells from C57BL/6 mice. Data are given as the fold change relative to *Rpl19* x1000. Histograms indicate the mean of three replicates and error bars indicate s.d. Data is representative of at least two independent experiments for each data point. **(d)** The relative GFP MFI (KO:WT) was calculated for iNKT cells and CD4$^+$ Tconv cells from naïve mice (black bars), or from mice 10 days after EAE induction (grey bars). **(e)** The percentage of iNKT (CD3$^+$CD1d-tet$^+$) cells present in the spleen, inguinal LN and thymus was quantified in groups of *Gpr65*$^{+/+}$ and *Gpr65*$^{gfp/gfp}$ mice by flow cytometry. No statistically significant difference was observed, data are representative of three independent experiments. **(f)** Wildtype and *CD1d*$^{-/-}$ mice were immunized with 50 μg MOG_{35-55}/incomplete Freund's adjuvant /*M.Tb*. Clinical scores were monitored for 24 days. Average clinical score is given for each group of mice. The data are pooled from four independent experiments, *CD1d*$^{-/-}$*Gpr65*$^{+/+}$: $n = 53$ and *CD1d*$^{-/-}$*Gpr65*$^{gfp/gfp}$: $n = 55$. No significant difference was observed by comparing the area under the curve values between the two groups by *t*-test.EAE, experimental autoimmune encephalomyelitis.

were therefore not tested for expression here. Investigating GPR65 expression on MAIT cells and other CD1-restricted cell subsets in humans will be informative as to the effects of GPR65 in human disease.

Novel GPCRs offer an attractive avenue for MS therapeutics. One of the most commonly prescribed oral disease-modifying drugs, Fingolimod (Gilenya), is a GPCR agonist. Several companies are pursuing GPR65 as

a therapeutic target in oncology and immunological diseases and an agonist molecules, effective *in vitro*, have been reported.[34,35] The data presented here shows that GPR65 plays a suppressive role in EAE and suggests that agonism of GPR65 could be investigated as a therapeutic strategy for demyelinating autoimmune disease.

METHODS

Mice

C57BL/6JAusb and B6.SJL-PtprcaPepcb/BoyJAusb (CD45.1 congenic) mice were obtained from Australian Bioresources (ABR; Mossvale, Australia) and B6.SJL-Ptprc (CD45.1 congenic), B6.129S7-RAG1 (*Rag1*$^{-/-}$) mice were obtained from the Animal Resource Centre (Perth, Australia). *Gpr65*^{gfp10} mice were purchased from JAX® (stock number 008577) and backcrossed to C57BL/6J mice ($n > 11$). To avoid genetic drift in experimental cohorts, heterozygotes were paired, then *Gpr65*$^{gfp/gfp}$ or *Gpr65*$^{+/+}$ homozygous F1 were selected for breeding, cohorts *Gpr65*$^{gfp/gfp}$ or *Gpr65*$^{+/+}$ F2 progeny were used in experiments. *2D2* TCR transgenic (2D2.Tg) mice[24] were supplied by A/Professor David Brown, The Westmead Institute, Australia. The two strains were intercrossed to generate the *2D2.Gpr65*^{gfp} *line*. *CD1d*$^{-/-}$ mice for breeding and B6.PL-*Thy1*^{a}/CyJ (Thy1.1) congenic mice were originally purchased from Jackson labs (stock numbers 003814 and 000406). All mice were backcrossed at least 10 times to C57BL/6J. Animals were housed in specific-pathogen free (SPF) conditions (ABR), Moss Vale, or within the BTF at the Garvan Institute. All animal procedures were approved by the Institutional Animal Care and Use Committee at The Garvan Institute/St. Vincent's Animal Experimentation Ethics Committee.

EAE

EAE was induced in 8–13 week old mice by immunizing mice subcutaneously with 100 μL of an emulsification containing 50 μg/mouse of myelin oligodendrocyte glycoprotein peptide amino acids 35-55 (MOG_{35-55}) (MEVGWYRSPFSRVVHLYR NGK; ProSpec-Tany Technogene Ltd.) in incomplete Freund's adjuvant supplemented with 400 μg mouse^{-1} heat killed *Mycobacterium tuberculosis* (*M.Tb*; H37RA, Difco). Mice were monitored daily for symptoms and were scored as follows: 0, no disease; 1, loss of tail tone; 2, tail paralysis; 3, hind limb weakness; 4, hind limb paralysis; and 5, hind limb paralysis and forelimb weakness. Mice were euthanized if they reached a score >4, according to Garvan Institute Ethics guidelines. All scoring was performed by researchers blinded to the genotype of the mice.

Bone marrow chimeras

One day prior to BM reconstitution, recipient female B6.SJL-Ptprc (CD45.1) congenic mice were irradiated with a split dose of 2 × 425 rads. Donor BM from *Gpr65*$^{+/+}$, *Gpr65*$^{gfp/gfp}$ and Thy1.1 congenic C57BL/6J mice was isolated and 10 × 10^6 total BM cells (5 × 10^6 of each) were injected i.v. into the irradiated recipients. Mice were monitored for signs of weight loss for 1 week. Reconstitution was assessed after 6 weeks by tail bleed, and mice were used for studies after at least 8 weeks of reconstitution.

Antibodies, cytokines and flow cytometry

Flow cytometric staining was performed using panels of anti-mouse antibodies that included those against the following mouse proteins: CD4, CD3, CD45.2, Thy1.1, Thy1.2, CD24, NK1.1, CD44, CD62L, IFNγ, IL-10, IL-17, B220, Ly6G, CD11b (BD Biosciences) CD4, CD25, Foxp3, γδTCR, CD11c (eBiosciences). PE and BV421 labelled CD1d-αGalCer tetramer was purchased from Professor Dale Godfrey at the University of Melbourne. 7AAD (BD Biosciences) was used to exclude nonviable cells.

Briefly, cells were stained with desired surface markers for 30 min on ice. For intracellular staining, cells were stained first with surface markers followed by fixation and permeabilization (eBioscience). Flow cytometry data were acquired on the BD-CANTOII cytometer and analyzed using the FlowJo v9.7.7software (Tree Star).

Cell sorting

Cells were harvested under sterile conditions from spleen and lymph nodes (LN) by mechanical disruption and CD4$^+$ T cells enriched by magnetic depletion. Cells were incubated for 20 min with biotin-anti B220$^+$, biotin anti-CD11b$^+$, biotin anti-CD11c$^+$ and biotin anti-CD8α$^+$ antibodies (eBioSciences), rinsed and then incubated with anti-biotin microbeads (MACS; Miltenyi). Labeled cells were depleted using Miltenyi LS columns and magnets.

The antibody cocktail used for FACS of CD4$^+$ T cells and iNKT cells included PE-conjugated CD1d-αGalCer tetramer, PerCP Cy5.5 anti-CD62L, PE Cy7 anti-CD3, APC Cy7 anti-CD44, eFluor450 anti-CD4. Cells were sorted using a BD FACS Aria II at the Garvan Institute Flow Cytometry facility. Purity of all samples exceeded 95% for all populations.

Adoptive transfer of 2D2 TCR transgenic cells

Splenocytes were isolated from 2D2.Tg *Gpr65*$^{+/+}$ and 2D2.Tg *Gpr65*$^{gfp/gfp}$ mice and CD4$^+$ T cells magnetically enriched as above. The proportion of 2D2.Tg cells in each sample was determined by flow cytometry using anti-CD4 and anti-V-beta 11 antibodies.

For EAE experiments, 2.5 × 10^5 2D2.Tg CD4$^+$ T cells were transferred into CD45.1 recipient mice by i.v. injection and EAE induced by immunization as described, on the same day.

For analysis of proliferation, cells were labeled with Cell Trace™ Violet (CTV; Invitrogen Molecular Probes), counted and 2D2.Tg *Gpr65*$^{+/+}$ and 2D2.Tg *Gpr65*$^{gfp/gfp}$ cells mixed to achieve equal numbers of 2D2.Tg CD4$^+$ T cells. Each WT.CD45.1 recipient mouse received a total of 5 × 10^5 2D2.Tg CD4$^+$ T cells. Recipients were simultaneously immunized to induce suboptimal EAE, as described above (+MOG35-55) and one mouse was left as an unimmunized control (-MOG35-55).

In vitro activation of CD4+ T cells

Naïve $CD4^+$ T cells ($CD4^+CD62L^+CD44^+$) pooled from spleen and iLN of >2 $Gpr65^{+/+}$ or >2 $Gpr65^{gfp/gfp}$ mice were sorted to >99% purity. Cells were left untreated or stimulated in RPMI based complete media at a starting pH of 7.3 with 1 μg mL^{-1} anti-CD3 alone (αCD3) or along with anti-CD28 (αCD3 + αCD28) for 48 h.

RNA preparation and RT-PCR

Wildtype T cells and iNKT cells from C57BL/6 mice were sorted from pooled spleen and LN ($n = 5$) to >95% purity as follows: $CD4^+$ naïve ($CD1dtet^-CD4^+CD62L^+CD44^-$), $CD4^+$ central memory ($CD1dtet^-$ $CD4^+CD62L^+CD44^+$), $CD4^+$ effector memory ($CD1dtet^-$ $CD4^+CD62L^-CD44^+$), $CD8^+$ naïve ($CD1dtet^-CD8^+CD62L^+CD44^-$) and iNKT ($CD3^+CD1dtet^+$). RNA was prepared using the RNeasy Plus kit (Qiagen, Hilden, Germany) following the manufacturers instructions. Complementary DNA (cDNA) was prepared using SuperScript III (Invitrogen, Carlsbad, CA, USA) reverse transcriptase with Oligo-dT and random hexamers. RT-PCR primers were designed using Roche UPL Primer assay design centre and ordered from Applied Biosystems. RT-PCR analysis was conducted on cDNA using primer/probe mix in LightCycler Mastermix as per manufacturers instructions (Roche, Mannheim, Germany). The relative abundance of cDNA was determined in triplicate using the LightCycler480® (Roche Applied Science). Gene expression was normalized to the housekeeping gene ribosomal protein L19 (*Rpl19*). Murine *Gpr65* primers: Forward: TTCAGTCTGCCTGCATCAGT, Reverse CGGGAGGGGTATTTAGTCCTT, UPL Probe #76. Murine *Rpl19* primers: Forward CTCGTTGCCGGAAAAACA, Reverse TCATCCAGGTCACCTTCTCA, UPL probe #103. Relative units were calculated as the fold change relative to *Rpl19* x1000.

ACKNOWLEDGMENTS

We thank Dr Robert Salomon, Eric Lam and the Garvan Flow Facility for cell sorting; Australian BioResources for animal breeding and care; the Biological Testing Facility (Garvan Institute) for help with animal care; Professor Dale Godfrey and Marcin Ciula at the University of Melbourne for αGalCer CD1d-tetramer; Professor David Brown at Westmead Institute for 2D2 TCR Tg mice; Chia-Ling Chan, Daniel Roden and Ben Elsworth in the Cancer Division at the Garvan Institute of Medical Research for experiments that informed the project. This work was supported by an innovation grant from Multiple Sclerosis Research Australia (11-022). MB is a recipient of a Career Development Fellowship from the National Health and Medical Research Council (NHMRC) of Australia (1031277).

CONFLICT OF INTEREST

The authors declare no competing financial interests.

REFERENCES

1. Tang XL, Wang Y, Li DL, Luo J, Liu MY. Orphan G protein-coupled receptors (GPCRs): biological functions and potential drug targets. *Acta Pharmacol Sin* 2012; **33**: 363–371.
2. Beecham AH, Patsopoulos NA, Xifara DK, *et al.* Analysis of immune-related loci identifies 48 new susceptibility variants for multiple sclerosis. *Nat Genet* 2013; **45**: 1353–1360.
3. Sawcer S, Hellenthal G, Pirinen M, *et al.* Genetic risk and a primary role for cell-mediated immune mechanisms in multiple sclerosis. *Nature* 2011; **476**: 214–219.
4. Barrett JC, Clayton DG, Concannon P, *et al.* Genome-wide association study and meta-analysis find that over 40 loci affect risk of type 1 diabetes. *Nat Genet* 2009; **41**: 703–707.
5. International Genetics of Ankylosing Spondylitis C; Cortes A, Hadler J, *et al.* Identification of multiple risk variants for ankylosing spondylitis through high-density genotyping of immune-related loci. *Nat Genet* 2013; **45**: 730–738.
6. Franke A, McGovern DP, Barrett JC, *et al.* Genome-wide meta-analysis increases to 71 the number of confirmed Crohn's disease susceptibility loci. *Nat Genet* 2010; **42**: 1118–1125.
7. Jostins L, Ripke S, Weersma RK, *et al.* Host-microbe interactions have shaped the genetic architecture of inflammatory bowel disease. *Nature* 2012; **491**: 119–124.
8. Okada Y, Wu D, Trynka G, *et al.* Genetics of rheumatoid arthritis contributes to biology and drug discovery. *Nature* 2014; **506**: 376–381.
9. Lassen KG, McKenzie CI, Mari M, *et al.* Genetic Coding Variant in GPR65 Alters Lysosomal pH and Links Lysosomal Dysfunction with Colitis Risk. *Immunity* 2016; **44**: 1392–1405.
10. Radu CG, Cheng D, Nijagal A, *et al.* Normal immune development and glucocorticoid-induced thymocyte apoptosis in mice deficient for the T-cell death-associated gene 8 receptor. *Mol Cell Biol* 2006; **26**: 668–677.
11. Onozawa Y, Komai T, Oda T. Activation of T cell death-associated gene 8 attenuates inflammation by negatively regulating the function of inflammatory cells. *Eur J Pharmacol* 2011; **654**: 315–319.
12. Nagasaka A, Mogi C, Ono H, *et al.* The proton-sensing G protein-coupled receptor T-cell death-associated gene 8 (TDAG8) shows cardioprotective effects against myocardial infarction. *Sci Rep* 2017; **7**: 7812.
13. Le LQ, Kabarowski JH, Weng Z, *et al.* Mice lacking the orphan G protein-coupled receptor G2A develop a late-onset autoimmune syndrome. *Immunity* 2001; **14**: 561–571.
14. Wang JQ, Kon J, Mogi C, *et al.* TDAG8 is a proton-sensing and psychosine-sensitive G-protein-coupled receptor. *J Biol Chem* 2004; **279**: 45626–45633.
15. Ishii S, Kihara Y, Shimizu T. Identification of T cell death-associated gene 8 (TDAG8) as a novel acid sensing G-protein-coupled receptor. *J Biol Chem* 2005; **280**: 9083–9087.
16. Friese MA, Craner MJ, Etzensperger R, *et al.* Acid-sensing ion channel-1 contributes to axonal degeneration in autoimmune inflammation of the central nervous system. *Nat Med* 2007; **13**: 1483–1489.

17. Bitsch A, Bruhn H, Vougioukas V, *et al.* Inflammatory CNS demyelination: histopathologic correlation with in vivo quantitative proton MR spectroscopy. *AJNR Am J Neuroradiol* 1999; **20**: 1619–1627.
18. Kottyan LC, Collier AR, Cao KH, *et al.* Eosinophil viability is increased by acidic pH in a cAMP- and GPR65-dependent manner. *Blood* 2009; **114**: 2774–2782.
19. Mogi C, Tobo M, Tomura H, *et al.* Involvement of proton-sensing TDAG8 in extracellular acidification-induced inhibition of proinflammatory cytokine production in peritoneal macrophages. *J Immunol* 2009; **182**: 3243–3251.
20. Radu CG, Nijagal A, McLaughlin J, Wang L, Witte ON. Differential proton sensitivity of related G protein-coupled receptors T cell death-associated gene 8 and G2A expressed in immune cells. *Proc Natl Acad Sci USA* 2005; **102**: 1632–1637.
21. Mosenden R, Tasken K. Cyclic AMP-mediated immune regulation–overview of mechanisms of action in T cells. *Cell Signal* 2011; **23**: 1009–1016.
22. Bruckener KE, el Baya A, Galla HJ, Schmidt MA. Permeabilization in a cerebral endothelial barrier model by pertussis toxin involves the PKC effector pathway and is abolished by elevated levels of cAMP. *J Cell Sci* 2003; **116** (Pt 9): 1837–1846.
23. Gaublomme JT, Yosef N, Lee Y, *et al.* Single-Cell Genomics Unveils Critical Regulators of Th17 Cell Pathogenicity. *Cell* 2015; **163**: 1400–1412.
24. Bettelli E, Pagany M, Weiner HL, Linington C, Sobel RA, Kuchroo VK. Myelin oligodendrocyte glycoprotein-specific T cell receptor transgenic mice develop spontaneous autoimmune optic neuritis. *J Exp Med* 2003; **197**: 1073–1081.
25. Ryder C, McColl K, Zhong F, Distelhorst CW. Acidosis promotes Bcl-2 family-mediated evasion of apoptosis: involvement of acid-sensing G protein-coupled receptor Gpr65 signaling to Mek/Erk. *J Biol Chem* 2012; **287**: 27863–27875.
26. Godfrey DI, Rossjohn J. New ways to turn on NKT cells. *J Exp Med* 2011; **208**: 1121–1125.
27. Kieper WC, Troy A, Burghardt JT, *et al.* Recent immune status determines the source of antigens that drive homeostatic T cell expansion. *J Immunol* 2005; **174**: 3158–3163.
28. Malik S, Want MY, Awasthi A. The Emerging Roles of Gamma-Delta T Cells in Tissue Inflammation in Experimental Autoimmune Encephalomyelitis. *Front Immunol* 2016; **7**: 14.
29. Treiner E, Liblau RS. Mucosal-associated invariant T cells in multiple sclerosis: the jury is still out. *Front Immunol* 2015; **6**: 503.
30. Van Kaer L, Wu L, Parekh VV. Natural killer T cells in multiple sclerosis and its animal model, experimental autoimmune encephalomyelitis. *Immunology* 2015; **146**: 1–10.
31. Illes Z, Shimamura M, Newcombe J, Oka N, Yamamura T. Accumulation of Valpha7.2-Jalpha33 invariant T cells in human autoimmune inflammatory lesions in the nervous system. *Int Immunol* 2004; **16**: 223–230.
32. Miyazaki Y, Miyake S, Chiba A, Lantz O, Yamamura T. Mucosal-associated invariant T cells regulate Th1 response in multiple sclerosis. *Int Immunol* 2011; **23**: 529–535.
33. Novak J, Lehuen A. Mechanism of regulation of autoimmunity by iNKT cells. *Cytokine* 2011; **53**: 263–270.
34. Onozawa Y, Fujita Y, Kuwabara H, Nagasaki M, Komai T, Oda T. Activation of T cell death-associated gene 8 regulates the cytokine production of T cells and macrophages in vitro. *Eur J Pharmacol* 2012; **683**(1–3): 325–331.
35. Huang XP, Karpiak J, Kroeze WK, *et al.* Allosteric ligands for the pharmacologically dark receptors GPR68 and GPR65. *Nature* 2015; **527**: 477–483.

SUPPORTING INFORMATION

Additional Supporting Information may be found online in the supporting information tab for this article.